

## Effects of in-situ annealing processes of GaAs(100) surfaces on the molecular beam epitaxial growth of InAs quantum dots

V.H. Méndez-García, A. Lastras-Martínez, A.Yu Gorbachev, V.A. Mishurnyi, F. de Anda  
*Instituto de Investigación en Comunicación Óptica and Facultad de Ingeniería, Universidad Autónoma de San Luis Potosí,  
 Av. Karakorum 1470, Lomas 4<sup>a</sup>. Sección, San Luis Potosí, S.L.P., México 78210*

M. López-López, M. Calixto-Rodríguez  
*Physics Department, Centro de Investigación y de Estudios Avanzados del IPN  
 Apartado Postal 14470, Mexico, D.F., México  
 (Recibido: 1de abril de 2005; Aceptado: 11 de mayo de 2005)*

We studied the growth of self-assembled InAs quantum dots (QDs) on GaAs (100) surfaces subjected to an in-situ annealing treatment. The treatment consists in exposing the GaAs buffer layer surface at a high temperature for a few seconds with the As<sub>4</sub>-shutter closed. The exposure of GaAs at high temperature leads to the formation of nanometric scale pits plus a Ga-rich surface. The annealing modifies in such a way the GaAs surface that the strain mediated transition from two- to three-dimensional InAs growth takes place at a much larger InAs thickness than the obtained under standard conditions. Moreover, the resulting QDs obtained at the equivalent InAs thickness of 3.4 monolayers (MLs) on the annealed GaAs surfaces presented a smaller size dispersion as compared with the conventionally grown QDs. The photoluminescence (PL) emission spectra corresponding to the samples subjected to the in-situ thermal treatment observed a reduction in the full width at half maximum (FWHM) and a clear correlation between the dots size increase and the emission peak red-shift. The new-flanged nucleation propitiated by the annealing process was explained in terms of a generation of an intermediated InGaAs thin film created by Ga-clusters on an atomically rough surface and the impinging In atoms.

*Keywords:* Nanostructures; Quantum dots; Molecular beam epitaxy; Semiconducting III-V materials

### 1. Introduction

The development and optimization of zero-dimensional structures where the 3D quantum confinement imposed on the electron and hole motion leads to strongly modified electronic and optical properties has attracted great interest for the future nano-scale optoelectronic devices, such as single-electron transistors and quantum dots lasers as well as other fundamental research. Self-assembled methods such as droplet epitaxy [1,2] and the Stranski-Krastanov (S-K) growth mode [3-5] have been proposed for the growth of these zero-dimensional semiconductor structures also known as quantum dots (QDs). The droplet epitaxy method is based on V-column element incorporation into the III-column element droplets deposited on III-V (or II-VI) compound semiconductor substrates [6]. However, QDs grown employing this method have exhibited large size as long as low density, making difficult their application in optoelectronic devices. On the other hand, the S-K growth method is based on strain that arises from the lattice mismatch between the epilayer and the substrate. The growth of InAs on GaAs is a typical example, where the lattice mismatch between InAs and GaAs is close to 7%. Dislocation-free high-density coherent 3D islands of InAs are self-assembled on the GaAs surface accompanied with a 2D wetting layer. The islands grown by this way exhibit smaller sizes and higher densities than those obtained employing the droplet epitaxy method. Nevertheless, the self-assembled islands appear in such a spontaneous way that makes difficult to obtain uniform

island sizes as well as to control their arrangement on the surface, limiting their application to potential devices and complicating the studies on their fundamental physics. Despite many works have been devoted to the achievement of regular in-plane spatial distributions and sufficiently uniform island sizes employing the S-K growth mode [7-11], these factors remain as challenging issues until now.

In the work reported here, we propose an in-situ procedure to improve the size distribution of the dots arrays. Our approach is to subject the GaAs buffer layers to an annealing process under no As-flux during a short time interval before starting the InAs QDs growth. The GaAs surface treatment performed at high temperature under no As-flux was made with the aim to change the chemical and mechanical conditions of the GaAs prior to the InAs deposition. The atomic force microscopy (AFM) images showed an improved morphology and a decrease in size dispersion for the InAs QDs grown on the GaAs surfaces subjected to the thermal treatments. PL emission spectra of the treated samples showed a diminution in their broadening as well as a red-shift in the emission peak due to the QDs size increase.

### 2. Experimental

The growths were performed in a RIBER-32 molecular beam epitaxy (MBE) system employing GaAs (100)  $\pm$  0.2° substrates previously etched in an H<sub>2</sub>SO<sub>4</sub>: H<sub>2</sub>O<sub>2</sub>: H<sub>2</sub>O

\*Corresponding author: Tel: +52 44 48 25 01 83, Fax: +52 44 48 25 01 98  
 e-mail: vmendez@cactus.iico.uaslp.mx

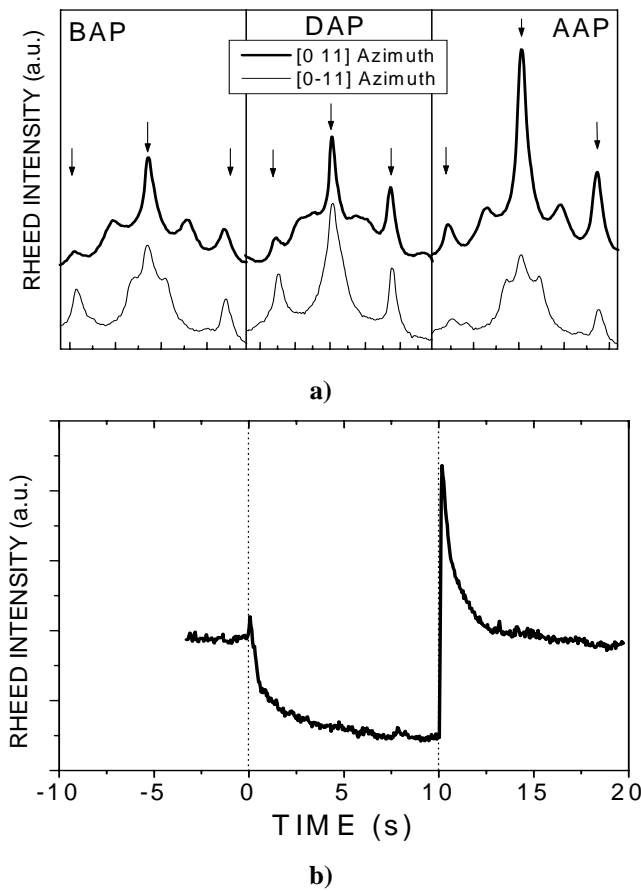


**Figure 1.** a) Intensity profiles taken from the RHEED patterns along  $[0\bar{1}1]$  and  $[011]$  azimuths at different stages of the GaAs surface treatment at  $650^\circ\text{C}$ : before the annealing process (BAA), when the  $\text{As}_4$  shutter was closed (DAP), and after the annealing (AAP). b) RHEED intensity oscillations observed along  $[0\bar{1}1]$  direction of the  $(0\bar{1})$  diffracted rod during the annealing process.

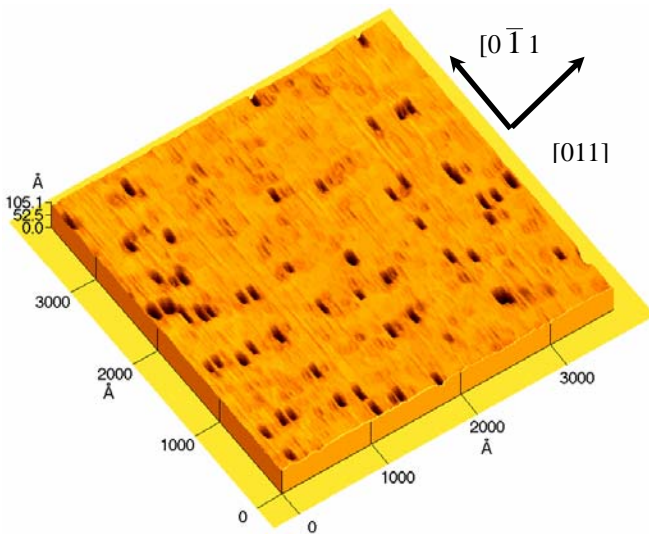


**Figure 2.** AFM image of the GaAs surface after the annealing process, Sample S481.

(5:1:1) solution. The thin oxides layer was removed by thermal desorption at  $585^\circ\text{C}$  under As-flux in ultra high vacuum environment. Then, a  $0.5\ \mu\text{m}$ -thick GaAs buffer layer (BL) was grown at  $600^\circ\text{C}$  at the growth rate of  $0.5\ \mu\text{m/hr}$ . Then, we prepared several samples employing the following growth conditions. Sample S312 and S242 corresponds to conventional QDs growths where the InAs was deposited at  $500^\circ\text{C}$  directly on the GaAs BL surface. The InAs equivalent thickness was 2.1 and 3.4 MLs for Samples S312 and S242, respectively. For Sample S481, after the GaAs-BL growth the substrate temperature was increased up to  $650^\circ\text{C}$  under  $\text{As}_4$  flux. Once reaching this temperature the  $\text{As}_4$ -shutter was closed. After 10 s the  $\text{As}_4$ -flux was reestablished again and the substrate was cooled down in order to remove the sample from the MBE system. Throughout the GaAs surface treatment the MBE growth chamber Arsenic background pressure was  $8.2 \times 10^{-8}$  Torr. For the other samples, after the annealing process described for S481 the substrate temperature was lowered to  $500^\circ\text{C}$  and the equivalent of 2.1 ML and 3.4 ML of InAs were deposited for S323 and S314, respectively. The InAs deposition was carried out for all the samples at the growth rate of 0.1 ML/sec. The samples surface was characterized by AFM operated in contact and tapping mode and 15K PL measurements were performed with a 514 nm wavelength Ar-laser as the excitation source.

### 3. Results and Discussion

We shall start the discussion presenting the analysis of the annealing process. Fig. 1(a) shows the RHEED intensity profiles observed along  $[011]$  and  $[0\bar{1}1]$  azimuths at different stages of the GaAs surface annealing process at  $650^\circ\text{C}$ : before, during and after the annealing process are labeled as BAP, DAP and AAP, respectively. The arrows indicate the diffractions rods  $(0\bar{1})$ ,  $(00)$  and  $(01)$ . Fig. 1(b) shows the  $(0\bar{1})$  diffracted rod intensity behavior observed along the  $[0\bar{1}1]$  azimuth during the annealing. It is worth to mention that throughout the GaAs BL growth and just before that the  $\text{As}_4$  shutter was closed at  $650^\circ\text{C}$ , it was observed an As-rich  $2 \times 4$  surface reconstruction as indicated by the  $\frac{1}{2}$ - and  $\frac{1}{4}$ -order diffraction rods in Fig. 1(a) -BAP. When the  $\text{As}_4$  shutter was closed, the spot intensity decreased abruptly (see Fig. 1(b)). The half- and quarter-order diffracted beams experienced a decrease in their intensity and the  $2 \times 4$  pattern turned into a blurred  $2 \times 1$  reconstruction. Immediately after the  $\text{As}_4$  flux was reestablished again, the spot intensity changed and the  $2 \times 4$  pattern was reestablished. The observed changes are mainly attributed to the As evaporation from the surface since at a temperature of  $650^\circ\text{C}$  the As evaporation rate is so elevated that it leaves a large number of vacancies letting exposed the underlying Ga atoms [12]. Actually, the  $(2 \times 1)$  surface reconstruction observed during the thermal treatments has been associated to a Ga-rich reconstruction, which leads on

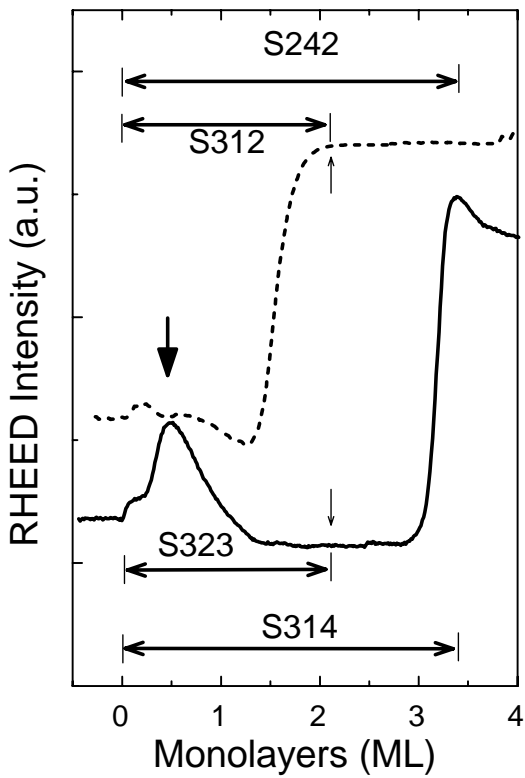


**Figure 3.** RHEED transmission spot intensity oscillations observed along  $[0\bar{1}1]$  direction when the InAs deposition was performed on the annealed (solid line) and not-annealed (dashed line) GaAs surfaces. The insets show the RHEED patterns obtained after the growth of 2.1 InAs MLs.

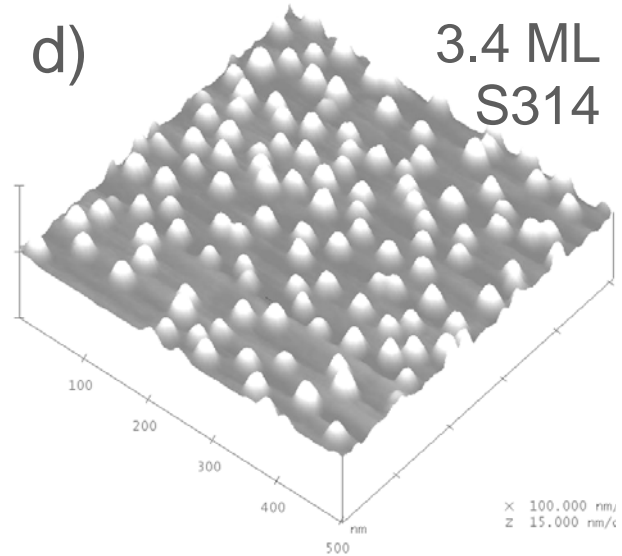
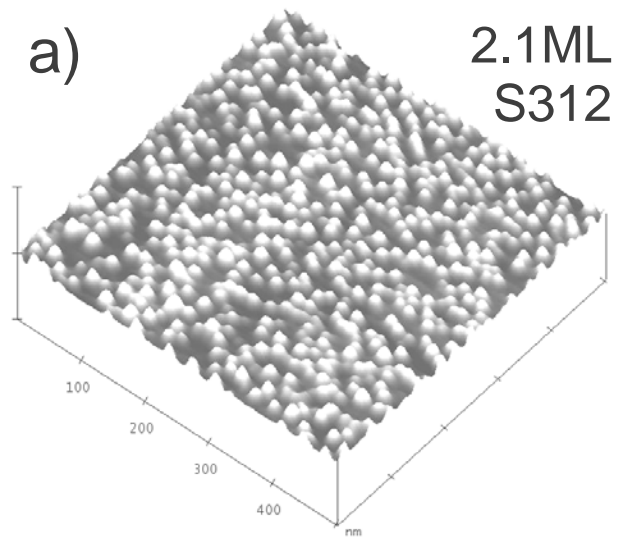
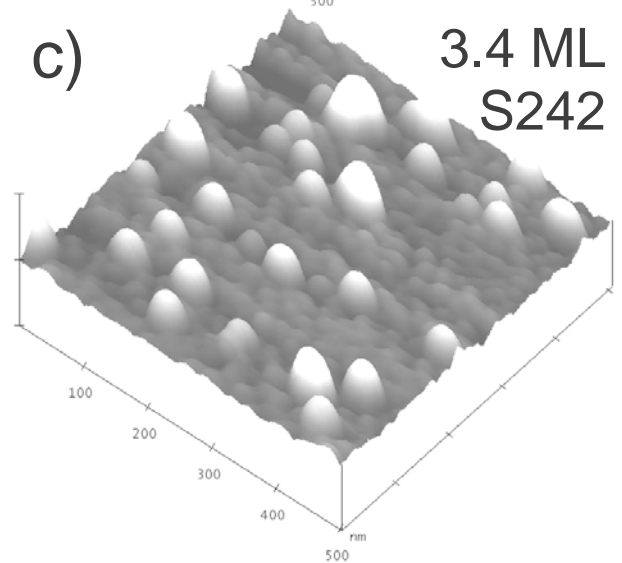
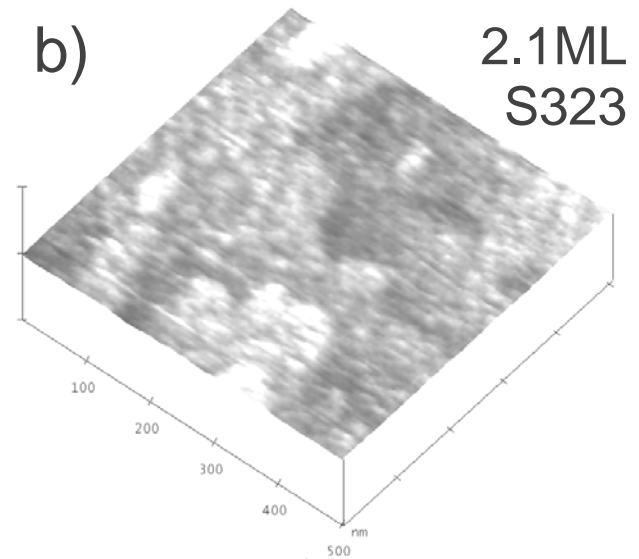


**Figure 4.** AFM images after the growth of InAs (a), (c) on a GaAs surface subjected to no annealing process; (b), (d) on annealed GaAs surfaces. The InAs equivalent thickness of each sample is indicated in the figure.

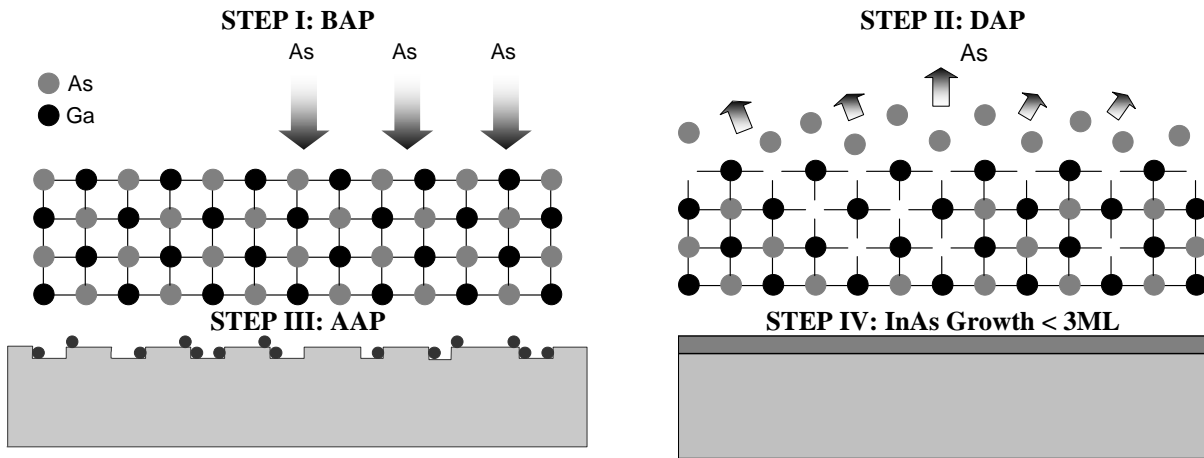


Figure 5. Schematic drawings showing the model for the InAs QDs formation on GaAs surface with annealing process.

nonmetallic and nonpolar surface [13]. The above discussion is very important in our experiments because the nonpolarity suggests the creation of clusters on the surface due to the high surface tension of the Ga atoms. At the moment the  $As_4$  shutter was reopened, no oscillations of the specular beam intensity are observed in Fig. 1(b) indicating that there was no GaAs overgrowth. Besides, the sudden evaporation of As occurred at high temperature leads on an atomically rough surface. Fig. 2 shows an AFM image measured in tapping mode of the GaAs surface after the annealing process, Sample S481, where a high density of nanometric scale pits can be observed. The pits density is approximately  $3 \times 10^{10}$  pits/cm<sup>2</sup>. Thus, Ga droplets (for Samples S314 and S323) could have rested on the atomically rough surface prior to the InAs deposition, contributing in this way to the remarkable changes observed for the QDs as will be explained later.

During the InAs deposition we sensed the temporal evolution of the RHEED transmission spot intensity (where the  $v$ -chevron spots appear) in order to get information of the islanding process. Fig. 3 shows the RHEED transmission spot behavior observed along the  $[0 \bar{1} 1]$  direction when the InAs overgrowth was performed on the different GaAs surfaces. The thickness for each sample is indicated by horizontal arrows. From the very early stages of InAs growth (InAs equivalent thickness less than one ML) the RHEED features presented noticeable changes showing as a general characteristic a peak that appeared just when the In shutter was opened. The peak, indicated with a vertical arrow in Fig. 3, increased considerably for the InAs deposition on GaAs surfaces subjected to the thermal treatment at high-temperature. The diversity of kinetic processes occurred at the early stages of growth makes difficult to state the origin of the observed differences. Nevertheless, it is clear that the formation of the wetting layer has been quite affected by the GaAs surface annealing. From the RHEED intensity response curves shown in Fig. 3 it can be observed that the initial growth conditions were crucial in the self-assembling by S-K growth mode since the 2D-3D growth mode transition

was reached at approximately 1.7 InAs ML only for Samples S312 and S242 in good agreement with other publications [10,14]. On the contrary, for the thermal treated Sample S314 it was reached up to  $\sim 3.0$  ML. Moreover, the insets in Fig. 3 show the RHEED patterns obtained at the end of the deposition of 2.1 InAs ML. While for Samples S312 and S242 typical chevrons-like patterns associated to faceted growth of QDs are observed, streaky RHEED patterns characteristic from flat surfaces for annealed Samples S314 and S323 are obtained.

The AFM images obtained from the grown samples are shown in Fig. 4. The scan range is  $500 \times 500$  nm<sup>2</sup> while the vertical scale is 10 nm. In Fig. 4(a) can be observed a typical AFM image obtained after depositing the equivalent of 2.1 ML of InAs on GaAs under standard conditions, Sample S312. The small dots exhibit a density of  $15 \times 10^{10}$  cm<sup>-2</sup> with a random size distribution, which is a usual characteristic of the Stranski-Krastanov growth mode. In contrast, Fig. 4(b) shows the AFM image obtained for Sample S323 after depositing the same 2.1 InAs ML employed for the former sample. However, at this time is observed a flat surface confirming the streaky RHEED pattern obtained at the end of this growth. Evidently, the annealing process performed under no As flux before the InAs growth changed considerably the surface since after 2.1 InAs MLs the growth was still pseudomorphic without the use of surfactants and under As-stable conditions. It is worth to mention that the 2D surface of Sample S323 could not correspond to pure InAs, but to a ternary alloy ( $In_xGa_{1-x}As$ ) as will be discussed later. When the InAs thickness is increased for the conventionally grown sample (Sample S242) the coalescence of QDs and subsequent formation of large islands is observed, see Fig. 4(c). On the contrary, the deposition of 3.4 ML of InAs on the annealed surface of Sample S314 resulted on the self-formation of QDs. Although the dots are still distributed randomly, they exhibit higher uniformity as well as the largest dimensions than the conventionally obtained QDs. The dots density is around  $5 \times 10^{10}$  cm<sup>-2</sup>. Obviously, the new dots morphology resulted from the annealing process at which the GaAs

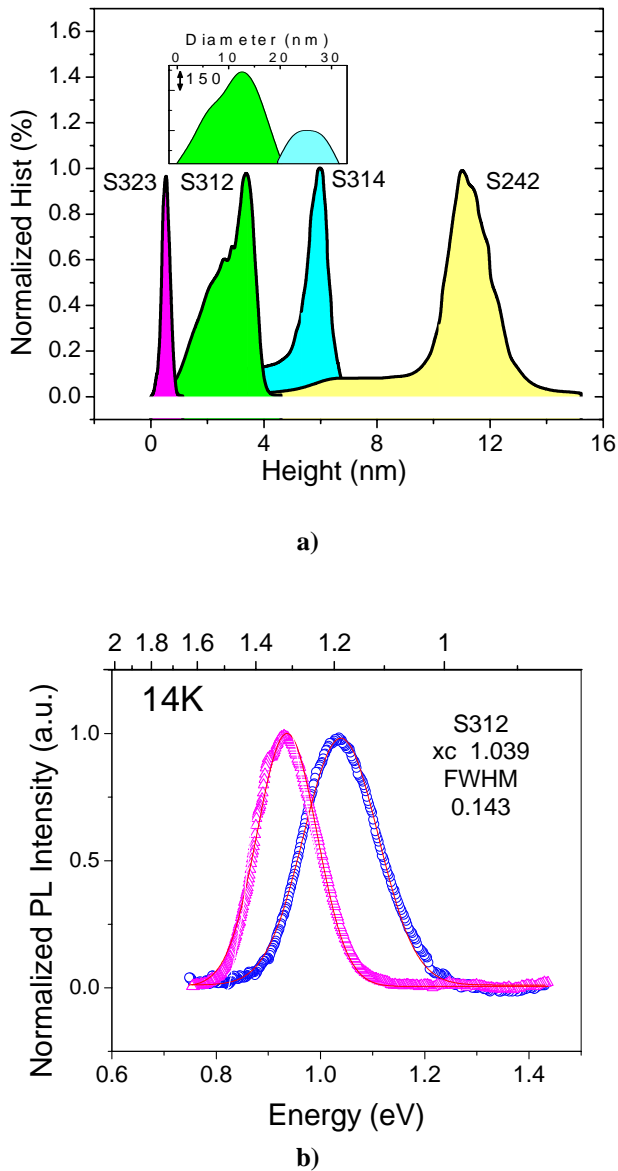


**Figure 6.** a) Heights distribution statistics obtained by AFM for the studied samples. The inset shows the QDs diameter histograms of Samples S312 and S314. b) Photoluminescence spectra obtained at 15 K.

surface of Sample S314 was subjected since QDs formation is strongly influenced by the early steps of growth, as previous reports affirm [15].

The AFM images evidence that InAs QDs arrays have been quite affected by the thermal treatment performed to GaAs surfaces. Fig. 5 shows schematically the growth process proposed on surfaces subjected to the annealing process without any As flux. Step I: the GaAs surface is maintained at 650°C under As flux. Step II: During the thermal treatments performed at a temperature of 650°C, As evaporation from the topmost layers occurred leaving a large number of vacancies and letting exposed the underlying Ga atoms as confirmed by the (2×1) RHEED pattern. Step III: The annealing process resulted in a pits

featured GaAs surface, and since Ga atoms exhibit a very high surface tension, it is very possible the formation of Ga clusters or droplets on the surface. Presumably, these Ga-clusters are very close or within the observed pits. Step IV: When the InAs deposition was performed, the incoming In and As found these Ga rich regions and an  $\text{In}_x\text{Ga}_{1-x}\text{As}$  layer was grown smoothing out the surface. It is well known that  $\delta_{\text{eff}} = (1-X_{\text{Ga}}) \delta_{\text{InAs}}$ , where  $X_{\text{Ga}}$  is the Ga content that in this case is provided by the As desorption, and  $\delta_{\text{InAs}}$  the InAs/GaAs mismatch [16]. The effective lattice mismatch  $\delta_{\text{eff}}$  could have been reduced in this way and the 2D growth mode was preserved longer. When InAs deposition was continued on this 2D layer, the epilayer strain is increased due to the lattice mismatch and after depositing 3.0 InAs ML the 2D-3D transition is reached. This model is very plausible since it explains the flat surface obtained for Sample S323. Moreover, note that the pits density is very close to the QDs density for Sample S314. Then, these Ga-rich regions close to the pits could have acted as nucleation centers during the formation of the QDs.

Furthermore, it is important to mention that the InAs wetting layer thickness calculated for Samples S312 and S314 was about 1ML, considering a parabolic QDs shape with the dimensions obtained by AFM. These results suggest that the growth still follows the S-K mode, but it is strongly affected by the Ga clusters formation. However, in order to get an accurate measurement of the wetting layer from the samples as well as additional information about the QDs nucleation, further experiments like transmission electron microscopy (TEM) are necessary and are currently in progress.

Fig. 6(a) shows the islands height distribution as obtained by AFM. The histograms illustrate both the flat surface obtained for Sample S323 and the big islands observed for Sample S314. PL spectra taken at 15K are presented in Fig. 6(b). The energy positions of the PL peaks are 1.03 and 0.93 eV for Samples S312 and S314, respectively. No photoluminescence signals were obtained in this spectral region for other samples, confirming that there is no electronic confinement since no QDs appeared on Sample S323 and the islands are too big for Sample S242. Therefore, the further analysis is focused on Samples S312 and S314. The islands diameters histograms are shown in the inset of Fig. 6(a). The diameters histograms show clearly how the increasing of the dots dimensions goes along with a diminution in the dots density. QDs grown employing the typical procedure had an average height of  $2.9 \pm 1$  nm and diameters about  $12 \pm 3.1$  nm. The dots grown on the GaAs surface annealed at high-temperature have an average height of  $5.9 \pm 0.5$  nm and diameters about  $25 \pm 2.5$  nm. The standard deviations of the former parameters are taken as the FWHM of Gaussian fits performed to the curves of Fig. 6(a). It is observed that the relative diameter and height dispersion changed from above 26% for Sample S312, to below 10% for Sample S314. The former improvement in the QDs size was reflected on the PL emission of QDs. It was observed a diminution in the PL emission spectra broadening of

Sample S314 as a consequence of the QDs size uniformity improvement. Concerning the energy position in the PL spectra of the emission peaks it is evident that the increase of the dots sizes matches perfectly with the red-shift observed for Sample S314. Moreover, it was found that the red-shift magnitude depends on both, the high temperature treatment exposure time and of the amount of InAs deposited. Thus, by changing these growth parameters the results suggest the possibility of tailoring the QDs emission peak. Note that the emission wavelength of the treated samples is close to  $\sim 1.3\mu\text{m}$ , the wavelength where optical dispersion and lessening are minimized in optical data transmission systems. Therefore, this method would open new possibilities in the synthesis of lower frequency emitting devices based on QDs.

#### 4. Conclusions

InAs QDs growth was performed on GaAs surfaces subjected to in-situ annealing processes under no As flux. The thermal treatment creates a high density of nanoscale pits and causes the formation of Ga clusters on the surface preserving the InAs pseudomorphic growth regime at larger thickness. Moreover, when the InAs QDs appeared on this surface, they observed a considerable improvement on their arrangement as well as a significant reduction in their size dispersion. The increase of the dots dimensions and size homogeneity was revealed as an energy red-shift as well as in narrower broadenings for the PL emission spectra of the dots grown on the GaAs surfaces subjected to the annealing process.

#### Acknowledgments

The authors would like to express their thanks to the technical staff members: N. Saucedo-Zeni, B.E. Torres-

Loredo and R. Fragoso. This work was partially supported by CONACyT-Mexico, FAI-UASLP, PROMEP-SESIC.

#### References

- [1] C.D. Lee, C. Park, H.J. Lee, S.K. Noh, K.S. Lee, S.J. Park, *Appl. Phys. Lett.* **73**, 2615 (1998).
- [2] Y. Hasegawa, T. Egawa, T. Jimbo, M. Umeno, *Appl. Phys. Lett.* **68**, 523 (1996).
- [3] J.M. Moison, F. Houzay, F. Barthe, L. Leprince, E. Andre, O. Vatel, *Appl. Phys. Lett.* **64**, 196 (1994).
- [4] M. Grundmann, O. Stier, D. Bimberg, *Phys. Rev. B* **52**, 11969 (1995).
- [5] J. Oshinowo, M. Nishioka, S. Ishida, Y. Arakawa, *Appl. Phys. Lett.* **65**, 1421 (1994).
- [6] T. Mano, K. Watanabe, S. Tsukamoto, H. Fujioka, M. Oshima, N. Koguchi, *J. Crystal Growth* **209**, 504 (2000).
- [7] P.B. Joyce, T.J. Krzyzewski, G.R. Bell, T.S. Jones, E.C. Le Ru, and R. Murray, *Phys. Rev. B* **64**, 235317(2001).
- [8] D.L. Huffaker and D.G. Deppe, *Appl. Phys. Lett.* **73**, 520 (1998).
- [9] P.B. Joyce, T.J. Krzyzewski, G.R. Bell, T.S. Jones, S. Malik, D. Childs, R. Murray, *J. Crystal Growth* **227-228**, 1000 (2001).
- [10] G.S. Solomon, J.A. Trezza, J.S. Harris Jr., *Appl. Phys. Lett.* **66**, 3161 (1995).
- [11] S. Kiravittaya, Y. Nakamura, O.G. Schmidt, *Physica E* **13**, 224 (2002).
- [12] M. López, Y. Takano, K. Pak and H. Yonezu, *Jpn. J. Appl. Phys.* **31**, 1745 (1992).
- [13] D.J. Chadi, *J. Vac. Sci. Technol. A* **5**, 1482 (1987).
- [14] P.B. Joyce, T.J. Krzyzewski, G.R. Bell, B.A. Joyce, T.S. Jones, *Phys. Rev. B* **58**, R15981 (1998).
- [15] B.F. Lewis, T.C. Lee, F.J. Grunthaler, A. Madhukar, R. Fernandez, and J. Maserjian, *J. Vac. Sci. Technol. B* **2**, 419 (1984).
- [16] Ch. Heyn and W. Hansen, *J. Crystal Growth* **251**, 140 (2003).